

# Contact Replacement for NMR Resonance Assignment

Fei Xiong<sup>a</sup>, Gopal Pandurangan<sup>b\*</sup> and Chris Bailey-Kellogg<sup>a\*</sup>

<sup>a</sup>Department of Computer Science, Dartmouth College, Hanover, NH 03755.

<sup>b</sup>Department of Computer Science, Purdue University, West Lafayette, IN 47907.

## ABSTRACT

**Motivation:** Complementing its traditional role in *structural* studies of proteins, nuclear magnetic resonance (NMR) spectroscopy is playing an increasingly important role in *functional* studies. NMR dynamics experiments characterize motions involved in target recognition, ligand binding, etc., while NMR chemical shift perturbation experiments identify and localize protein-protein and protein-ligand interactions. The key bottleneck in these studies is to determine the backbone resonance assignment, which allows spectral peaks to be mapped to specific atoms. This paper develops a novel approach to address that bottleneck, exploiting an available x-ray structure or homology model to assign the entire backbone from a set of relatively fast and cheap NMR experiments.

**Results:** We formulate *contact replacement* for resonance assignment as the problem of computing correspondences between a contact graph representing the structure and an NMR graph representing the data; the NMR graph is a significantly corrupted, ambiguous version of the contact graph. We first show that by combining connectivity and amino acid type information, and exploiting the random structure of the noise, one can provably determine unique correspondences in polynomial time with high probability, even in the presence of significant noise (a constant number of noisy edges per vertex). We then detail an efficient randomized algorithm and show that, over a variety of experimental and synthetic datasets, it is robust to typical levels of structural variation (1–2 Å), noise (250–600%) and missings (10–40%). Our algorithm achieves very good overall assignment accuracy, above 80% in  $\alpha$ -helices, 70% in  $\beta$ -sheets, and 60% in loop regions.

**Availability:** Our contact replacement algorithm is implemented in platform-independent Python code. The software can be freely obtained for academic use by request from the authors.

**Contact:** gopal@cs.purdue.edu; cbk@cs.dartmouth.edu

## 1 INTRODUCTION

Nuclear magnetic resonance (NMR) spectroscopy is playing an increasingly important role in studies of proteins beyond the determination of their three-dimensional structures. For example, since NMR is performed in solution, it can gather information regarding dynamics (Palmer III *et al.*, 1996; Kay, 1998) and structure-function relationships under varying conditions (Montelione *et al.*, 2000). Similarly, solution NMR is a vital tool in assessing ligand binding for drug development (Shuker *et al.*, 1996; Hajduk *et al.*, 1997) and can also help characterize protein-protein interactions (Chen *et al.*,

1993). These applications of NMR are significant even if the structure has already been determined by x-ray crystallography or a high quality homology model is available.

Unfortunately, the data collected in NMR studies are in terms of the resonance frequencies of the atomic nuclei, which are not readily predictable. “Resonance assignment” determines the previously unknown mapping between the atoms in the protein and the observed resonance frequencies, so that the information about binding, dynamics, etc. can be properly interpreted. Backbone resonance assignment has been well-studied within the context of structure determination (e.g., Bartels *et al.* (1997); Zimmerman *et al.* (1997); Moseley and Montelione (1999); Xu *et al.* (2000); Lin *et al.* (2002); Jung and Zweckstetter (2004); Vitek *et al.* (2005, 2006)). However, the standard protocols used in that context require much more (and more expensive) experimentation than is necessary for the dynamics and interaction studies mentioned above. While the standard protocols and assignment approaches could still be employed for those studies, using an available structure offers the potential to reduce the experimental complexity and circumvent traditional barriers to interpretation. Our goal is to develop computational techniques that enable assignment from a minimalist set of experiments that require only <sup>15</sup>N labeled sample rather than the much more expensive <sup>13</sup>C-<sup>15</sup>N labeling used in standard protocols.

Here we formulate the problem of assignment given a structure and minimalist NMR data as the *contact replacement problem* (Fig. 1). A contact graph representing a protein structure has vertices for the individual amino acid residues in the protein and edges between nearby pairs. A particular form of “interaction graph” representing NMR data has vertices for NMR-probed “pseudoresidues” (which correspond via an unknown mapping to the real residues), and edges between pairs that, if they were nearby, would explain the data. The NMR edges are essentially the contact edges, significantly corrupted by experimental noise and ambiguity (around 5 noisy edges per correct one). The contact replacement problem is then to uncover the correspondences between these graphs for a given protein.

The name “contact replacement” for our problem is inspired by the names for the analogous problems “molecular replacement” in x-ray crystallography (Rossman and Blow, 1962) and “nuclear vector replacement” in NMR (Langmead and Donald, 2004; Langmead *et al.*, 2004). In molecular replacement, initial data interpretation is aided by matching against available structural information from a related protein. Likewise, in nuclear vector replacement, residual dipolar coupling data are matched against predictions from an available structure (or high-quality model). Contact replacement and nuclear vector replacement are complementary, relying on different types of NMR data with different information content (distances vs.

\*to whom correspondence should be addressed

orientations). The contact replacement problem is related to threading (sequence-structure alignment), but for threading, residues are in sequential order for both the sequence and the structure, whereas here we have no information about the sequential order of the pseudoresidues.

Various versions of what we are calling here contact replacement have previously been studied. Our Hierarchical Grow-and-Match (HGM) algorithm (Xiong and Bailey-Kellogg, 2007) uses a branch-and-bound algorithm to find the complete ensemble of consistent correspondences between contact graphs and NMR graphs, and can handle significant noise and sparsity. However, due to the combinatorics of the problem and the branch-and-bound approach, HGM is effectively restricted to well-defined regions of secondary structure. The ST2NMR program (Pristovek et al., 2002) casts assignment given a 3D structure and NMR data as an optimization problem, and uses a Monte Carlo approach to find explanations of the data in terms of distances in the structure. While ST2NMR was shown to be effective for some test data, it requires very specific experimental set-ups and can provide no guarantees or insights into the information content of the data. We tested it on a number of different datasets, and found the accuracy to be fairly low and quite sensitive to the order of the input data (Xiong and Bailey-Kellogg, 2007). PEPMORPH (Erdmann and Rule, 2002) uses graph representations of the structure and data, but augments them with residual dipolar coupling data in order to compute matchings. Our earlier work on graph-based approaches to NMR assignment, Jigsaw (Bailey-Kellogg et al., 2000) and random graph algorithms (Bailey-Kellogg et al., 2005; Kamisetty et al., 2006), were able to effectively uncover secondary structure patterns; our random graph model enabled us to prove that the randomized methods have optimal performance in expected polynomial time. However, these approaches were all restricted to uncovering generic prototypes of secondary structure elements, rather than matching NMR data to an arbitrary three-dimensional structure.

**Contribution.** This paper presents the first *efficient* algorithm to solve the contact replacement problem for *entire* proteins. We first show that by combining connectivity and type, and by exploiting the random structure of the noisy edges and vertex labels, one can provably determine unique matchings in polynomial time with high probability, even in the presence of significant noise, i.e., a constant number of noisy edges per vertex. Since the NMR interaction graphs we are studying have up to 5 times as many noise edges as correct ones, the ability to handle this degree of noise is important. This result significantly improves over previous results on finding long paths in noisy NMR graphs (Bailey-Kellogg et al., 2005). We then detail a simple and efficient randomized algorithm that works very well in practice. To do so, we build upon our earlier work on random graph algorithms in NMR (Bailey-Kellogg et al., 2005; Kamisetty et al., 2006), which used connectivity information alone to uncover large, regular structures ( $\alpha$ -helices and  $\beta$ -sheets) in NMR graphs. We now integrate connectivity information with amino acid type information (ambiguous labels on the vertices) in order to uncover large corresponding fragments in NMR and contact graphs for complete structures. We significantly extend our *reuse* paradigm to efficiently uncover these correspondences. Instead of backtracking upon finding an inconsistency in a growing correspondence, the reuse approach seeks to maintain the (mostly good) structure by applying local fix-up rules to address just the source of the inconsistency. Our empirical results show that this approach is

quite effective in practice, relatively insensitive to both noise in the NMR graph and structural variation in the contact graph.

## 2 APPROACH

We first summarize the representations of the input contact graph and NMR interaction graph; for details see (Bailey-Kellogg et al., 2000, 2005; Kamisetty et al., 2006).

**Contact graph.**  $G^* = (V^*, E^*)$ , where  $V^*$  is a set of residue positions and  $E^*$  is a set of pairs of nearby residue positions. In particular, we place an edge when a pair of protons is within a specified distance threshold (say, 3, 4, or 5 Å). Each vertex  $v$  is labeled with its amino acid type,  $a(v)$ .

**NMR interaction graph.**  $G = (V, E)$ , where  $V$  is a set of *pseudoresidues* of unknown correspondence to the residues and  $E$  is a set of pairs of pseudoresidues that may have interacting protons (i.e., an interaction would explain a peak in the NOESY spectrum). Such a graph can be compiled from a set of four  $^{15}\text{N}$  spectra (HSQC, HNHA, TOCSY, and NOESY), and has a number of properties (Pristovek et al., 2002; Kamisetty et al., 2006; Xiong and Bailey-Kellogg, 2007):

- Each vertex is labeled with a *secondary structure type*, either  $\alpha$  or  $\beta$ , as determined from HNHA.
- Each vertex is labeled with a list  $\ell$  of *possible amino acid types*. We use here the classes output by RESCUE (Pons and Delsuc, 1999), which employs a two-level neural network to estimate amino acid type from proton chemical shifts. The first level associates a pseudoresidue with one of the ten type classes (IL, A, G, P, T, V, KR, FYWHDNC, EQM, and S) with very high accuracy (avg: 91.9%, min:88.1%); amino acids within a class are treated as indistinguishable.
- Each edge is labeled with an *interaction type* based on the chemical shift ranges. We use only  $\text{H}^{\text{N}}$  and  $\text{H}^{\alpha}$ , since a structure model’s side-chain atomic coordinates are usually less reliable, and we have not found their inclusion to aid the results.
- Each edge has a *match score*  $s$ , evaluating the quality of the edge as an explanation for the peak. Typical scoring rules (e.g., Zimmerman et al. (1997); Güntert et al. (2000); Vitek et al. (2004, 2005)) compare absolute or squared difference in chemical shift; except for noise (reasonably modeled as Gaussian), the correct edge should match exactly and have the best score. Here we score edges by error probability, i.e., how likely it is that an edge could be generated by noise. In this way, missing edges are naturally penalized since they contribute a score of zero. The score is thus  $-\log\left(1 - \frac{1}{\sqrt{2\pi}\sigma} \exp^{-\frac{\Delta(e)^2}{2\sigma^2}}\right)$  where  $\Delta(e)$  is the chemical shift difference for edge  $e$ , and  $\sigma$  is the standard deviation of chemical shift difference distribution.

Due to the nature of the  $^{15}\text{N}$  NOESY ( $\text{H}^{\text{N}}\text{-}^{15}\text{N}$  for one vertex and  $^1\text{H}$  for the other), the NMR interaction graph is directed. For consistency, we adopt the same convention for the contact graph.

We assume for simplicity that the contact graph is “correct”—it represents exactly those interactions that are physically present (thus its designation as  $G^* = (V^*, E^*)$ ), and all the errors are in the NMR graph. The NMR interaction graph  $G$  constructed from NMR

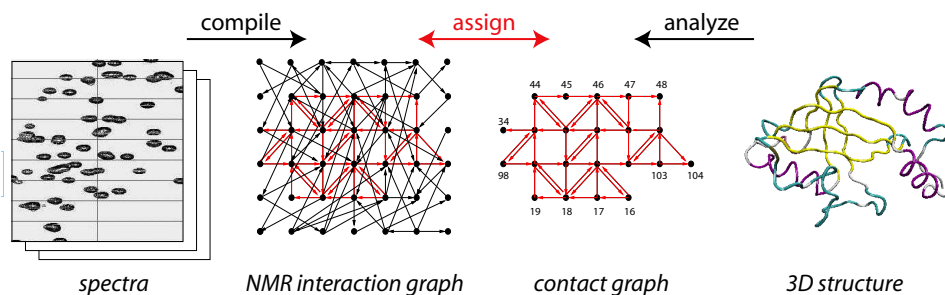


**Fig. 1.** Contact replacement. Both an existing three-dimensional structure and NMR data (based on the through-space NOESY experiment) are represented as graphs. The interaction graph representing the NMR data is essentially a corrupted, ambiguous version of the contact graph representing the structure. The goal is to uncover the correspondence.

data is substantially corrupted from  $G^*$ , and has an unknown vertex correspondence. We now formalize our problem in its cleanest form.

**PROBLEM 1 (Contact replacement).** *We are given a contact graph  $G^* = (V^*, E^*)$  and an NMR interaction graph  $G = (V, E)$ . The goal is to find a bijection  $m$  from  $V^*$  to  $V$  that matches amino acid classes and maximizes the score of the edges in  $E$  that correspond to edges in  $E^*$ . Formally, if  $m(v^*) = v$ , then we must have  $a(v^*) \in \ell(v)$ . The score is computed as  $\sum_{(e^*, e) \in c} s(e)$ , where the mapping  $c$  between  $E^*$  and  $E$  is induced by  $m$  as  $c = \{(u^*, v^*), (u, v) \mid (u^*, v^*) \in E^*, (u, v) \in E, m(u^*) = u, m(v^*) = v\}$ .*

One feature of proteins particularly relevant here is that they are made of chains of amino acids. Thus the contact graph has an embedded Hamiltonian path from N terminus to C terminus (in addition to numerous through-space edges connecting residues at any sequential distance). Ignoring missing edges, the NMR graph has a corresponding Hamiltonian path. Our analysis and randomized algorithm both make use of this property, by focusing on finding the Hamiltonian path while “bringing along” the additional edges for scoring purposes.

We note that the contact replacement problem is NP-hard in general, since it contains as a special case the following NP-hard problem: Given a unweighted Hamiltonian graph (undirected or directed)  $H$  find a Hamiltonian path in  $H$  (i.e., assuming that there are no constraints on vertex labels and all edge scores are the same). We note that the above problem remains NP-hard even when restricted to sparse Hamiltonian graphs, e.g., directed Hamiltonian graphs with maximum out-degree two (Plesnik, 1979) or undirected Hamiltonian graphs with degree at most three (Garey *et al.*, 1976). The problem has been shown hard to approximate in directed graphs: it is not possible to find paths even of superpolylogarithmic length in constant out-degree Hamiltonian graphs unless Satisfiability can be solved in subexponential time (Bjorklund *et al.*, 2003). For undirected Hamiltonian graphs, the best known algorithms give longer paths (e.g., of length  $n^{\Omega(1/\log \log n)}$ ) in Hamiltonian graphs in polynomial time (Feder and Motwani, 2005; Gabow, 2004; Feder *et al.*, 2002). We note that the above algorithmic results do not apply to our problem because we have additional information (amino acid classes) for the vertices. More importantly, NMR interaction graphs are not arbitrary graphs and indeed have a special structure as captured by the random graph model described next.

## 2.1 Random Graph Model for NMR Interaction Graph

In order to develop and analyze effective algorithms, we must consider and model the nature of the relationship between the ideal contact graph  $G^*$  and the observed NMR interaction graph  $G$ . We note that traditional  $G(n, p)$  random graph models (Bollobas, 2001) essentially add noise edges randomly and independently. However, the noisy edges in an NMR interaction graph are not arbitrarily distributed. Instead, *chemical shift degeneracy* is the key source of noise in these graphs, imposing a particular correlation structure among noise edges. We have developed a random graph model that properly captures the noise in NMR interaction graphs (Bailey-Kellogg *et al.*, 2005; Kamisetty *et al.*, 2006).

**DEFINITION 1 ( $M(G^*, w)$  random graph).** *The model  $M(G^*, w)$  “generates” a random graph from the (correct) graph  $G^*$ , where  $w$  is a parameter that determines the number of noisy edges generated per correct edge. Let  $\pi$  be a random permutation of  $V^*$ . Denote by  $\pi(v)$  the index of  $v \in V^*$  in the permutation. We then consider as ambiguous all vertices within a “window” of size  $w$  around a particular vertex. For each edge of  $G^*$ , additional edges are generated as follows. Consider an edge  $(u^*, v^*) \in E^*$ . Then for each  $u$  in the window of width  $w$  around  $\pi(u^*)$  (i.e.,  $|\pi(u^*) - \pi(u)| \leq w$ ), we add the edge  $(u, v^*)$  to the random graph.*

This model captures the way in which uncertainty in the data leads directly to ambiguity in the edges posited in an NMR graph. In particular, NMR spectra represent interactions between atoms as peaks in  $\mathbb{R}^2$  or  $\mathbb{R}^3$ , where each dimension indicates the coordinates (resonance frequencies, in units called “chemical shifts”) of one of the interacting atoms. Uncertainty in the measured chemical shifts of the protons thus leads to ambiguity in matches, and the construction of noise edges. When two vertices have atoms that are similar in chemical shift, they will tend to share edges—each edge for the one will also appear for the other. Since there is no systematic, global correlation between chemical shifts and positions of atoms in the primary sequence or in space, we simply model chemical shift similarity according to a random permutation. The model can be extended in order to generate synthetic data (e.g., incorporating edge scores, accounting for missing edges, etc.); see the Results section for our actual simulation testbed. We use this basic model in the next section to analyze the contact replacement problem.

For amino acid types, we assume a simple independent model for the purpose of analysis. (Of course, in practice we know the actual

amino acid types for the contact graph.) In particular, let  $A$  be the set of amino acid types and  $D$  be some fixed probability distribution over  $A$  (e.g.,  $1/20$  for each, or using empirically observed frequencies). Assume without loss of generality that for all  $a \in A$ , the probability that  $a$  is chosen,  $\Pr(a)$ , is greater than  $q$ , where  $q > 0$  is some fixed constant. We assume that a vertex is labeled by sampling independently at random from  $D$ .

### 3 THEORETICAL ANALYSIS AND IMPLICATIONS

We present a theoretical analysis to show that the contact replacement problem can be solved with high probability in polynomial time. For the analysis, we assume that the NMR interaction graph  $G = M(G^*, w)$  is generated from the correct contact graph  $G^* = (V^*, E^*)$  which is a Hamiltonian path of length  $n$  (= number of amino acids). For now, we assume no edge weights, no breaks, and no other sources of noise (additions and deletions); the result can be generalized. We also assume that for each vertex, the true amino acid type is in the amino acid class labeling the vertex, and that it is a non-trivial class, i.e., it is not  $A$  itself (refer to the model above). The contact replacement problem now reduces to finding whether there is a Hamiltonian path in  $G$  that is *equivalent* (defined below) to that of the Hamiltonian path  $G^*$ .

**DEFINITION 2 (equivalence).** *We say that a subgraph  $H = (V_1, E_1)$  of  $G$  is equivalent to a subgraph (i.e., subpath)  $H^* = (V_2, E_2)$  of  $G^*$ , denoted as  $H \equiv H^*$ , if and only if there is a bijection  $m : V_1 \rightarrow V_2$  such that for every  $v_1 \in V_1$ ,  $a(m(v_1)) \in \ell(v_1)$  and there is an edge  $e = (u_1, v_1) \in E_1$  iff there is an edge  $(m(u_1), m(v_1)) \in E_2$ .*

In the following, “with high probability (whp)” means with probability at least  $1 - 1/n^{\Omega(1)}$ , where  $n$  is the number of amino acids in the protein.

**THEOREM 1.** *Under our  $M(G^*, w)$  random graph model, if  $w = O(1)$ , then the contact replacement problem can be solved in polynomial time whp.*

**PROOF.** Without loss of generality, we will assume that  $|A| = 2$  ( $A$  is the set of amino acid types). The proof can easily be made to work without this restriction. The proof hinges on the following claim.

**Claim:** Fix a (sub)path  $P$  of length  $k = c \log n$  in  $G^*$ , where  $c > 0$  is a constant (fixed in the proof). Then the following hold whp.

- There is a unique subgraph  $H$  of  $G$ , such that  $H \equiv P$ , i.e., there is no other subgraph  $H'$  of  $G$  such that  $H' \equiv P$ .
- There is no other subgraph  $Q$  of  $G^*$  such that  $P \equiv Q$ .

We will first show (a).

Since  $G = M(G^*, w)$  (i.e., generated by our random graph model), we know that there exists a subgraph  $H$  of  $G$  such that  $H \equiv P$ . We now show that  $H$  is unique. Let the two amino acids be  $a$  and  $b$ , with probabilities of occurring  $p_a$  and  $1 - p_a$  respectively. Let  $q = \max\{p_a, 1 - p_a\}$ . By our assumption on the size of  $A$ ,  $q$  is a constant ( $< 1$ ). The path  $G^*$  induces a natural ordering of vertices of  $G$ . We bound the probability of finding another path (subgraph)

$H'$  of  $G$  that is equivalent to  $P$  by the following expression:

$$\Pr\{\exists H' \equiv P\} \leq \sum_{k'=0}^{k-1} n \binom{n}{k'} \left(\frac{w}{n}\right)^{k'} q^{k-k'}$$

The reasoning is as follows. Let  $k'$  be the number of noisy edges in  $H'$ ;  $k'$  can vary between 0 and  $k - 1$ , and hence we sum over all possibilities. The first term is the number of different ways of fixing the starting vertex. There are at most  $\binom{n}{k'}$  ways of choosing vertices from which the noisy edges emanate. The third term bounds the probability that the noisy edges form a path between them *with* the amino acid labels matching those of the corresponding vertices in  $P$ . The last term is the probability that the amino acid labels for the correct vertices match. We can bound the sum as follows (note that we take  $\infty^0 = 1$ ):

$$\begin{aligned} \Pr\{\exists H' \equiv P\} &\leq \sum_{k'=0}^{k-1} n \left(\frac{en}{k'}\right)^{k'} \left(\frac{w}{n}\right)^{k'} q^{k-k'} \\ &\leq \sum_{k'=0}^{k-1} n \left(\frac{ew}{k'}\right)^{k'} q^{k-k'} \end{aligned}$$

Plugging  $k = c \log n$ , the above sum is bounded by

$$\begin{aligned} \Pr\{\exists H' \equiv P\} &\leq n \sum_{k'=0}^{c \log n} \left(\frac{ew}{k'}\right)^{k'} q^{(c \log n) - k'} \\ &\leq n \sum_{k'=0}^{c \log n} \left(\frac{ew}{qk'}\right)^{k'} q^{c \log n} \\ &\leq n \sum_{k'=0}^{c \log n} \left(\frac{ew}{qk'}\right)^{k'} O(n^{c \log q}) \\ &\leq n \sum_{k'=0}^{c \log n} O(1) O(1/n^{c \log(1/q)}) \\ &\leq n \sum_{k'=0}^{c \log n} O(1/n^3) \\ &= O(1/n) \end{aligned}$$

if  $c$  is a sufficiently large constant.

We now show Claim (b). We bound the probability that there is some subgraph  $Q$  of  $G^*$  such that  $P \equiv Q$ :

$$\Pr\{\exists Q \equiv P\} \leq nq^k.$$

The first term in the bound is the number of different ways of fixing the starting vertex of  $Q$  and the second term bounds the probability that a particular  $Q$  is identical to  $P$ . If  $k = c \log n$ , for a sufficiently large constant  $c$ , the above probability is bounded by  $1/n$ .

Using the above claims we can design the following polynomial-time algorithm. The algorithm finds a subgraph  $H$  in  $G$  of length  $c \log n$  (where  $c$  is fixed in the above claim) such that it is equivalent to some subgraph  $P$  of  $G^*$ . Once such a subgraph is found, it will be a unique match in  $G^*$  whp (by the above claim). The algorithm then repeats this process until the full equivalent mapping is found. The subgraph  $H$  can be found by an exhaustive search, starting at some

vertex and examining all possible paths of length  $c \log n$ . There are only at most  $w^{c \log n} = O(n^{c \log w})$  (i.e., a polynomial number) of possible paths and hence the search can be done in polynomial time. One of these paths in  $G$  will be a unique match with a corresponding path in  $G^*$ .  $\square$

We note that the above theorem can be extended to the case when there are missing (correct) edges in the NMR graph  $G'$  as shown in the following corollary.

**COROLLARY 1.** *Suppose  $G$  contains a path  $P'$  of length at least  $c \log n$  (where  $c$  is as fixed in the above theorem) that is equivalent to a subgraph  $H^*$  of  $G^*$ . Then  $P'$  can be found and matched correctly with  $H^*$  whp.*

The above analysis shows that the contact replacement problem can be solved in polynomial time if  $w = O(1)$ , i.e., there is at most a constant number of noisy edges per vertex. This is significant for two reasons. First, in practice, typically the number of noisy edges per vertex is a constant (around 5). Second, if there is no amino acid information, the randomized algorithm of (Bailey-Kellogg *et al.*, 2005; Pandurangan, 2005) can find long paths (of length at least  $\Omega(n/\log n)$ ) in polynomial time only if the number of noisy edges per vertex is *at most one*. Our analysis here shows that *this threshold barrier can be surmounted* by using amino acid type information. Our experimental results validate this theoretical prediction.

## 4 METHODS

In practice, the simplified model and algorithm used in the analysis may not be fully applicable, in particular because some edges may be missing and some amino acid type information may be erroneous (the correct type for a contact graph vertex not included in the class for the corresponding NMR vertex). Such errors result in “breaks” in the correspondence between a contact graph and NMR graph. Thus we seek to find a set of disjoint paths (“fragments”) in the NMR graph that together match the Hamiltonian path in the contact graph. Given such an equivalence, we score *all* corresponding edges, including the non-sequential ones. By basing our algorithm on paths, we take advantage of our long-path result from the previous section, while by including all edges in the score, we take advantage of all available information to better control the search.

A key insight of our algorithm is that *in searching for good matchings, the best ones tend to share a lot of substructure*. (Our results below on assignment ambiguity, Fig. 5, illustrate.) In branching-based searches, such shared substructure can appear on many different branches, making exhaustive search very inefficient and causing backtracking to perform wasteful undoing and redoing. In contrast, we use more efficient local fixes to resolve inconsistencies and continue searching with most of the structure still intact.

Fig. 2 gives the pseudocode for our algorithm. The algorithm maintains (and fixes up) a single set  $F$  of fragments, with a mapping  $m$  to the contact graph that is always consistent (i.e., fragments do not overlap). Some fragments may not be mapped, meaning that under the current matching, they are considered noise. On each iteration, the algorithm sequentially extends one fragment, adding an NMR vertex that will correspond to the next residue position in the sequence. Several things could happen upon growing to that vertex; see Fig. 3. In the simplest case, the algorithm picks up an unmatched NMR vertex (and its fragment) and simply extends the matching. However, it may run into a conflict and need to fix up the current matching. If a fragment wants to grow to a vertex in the middle of another fragment, then the other fragment is split at the point of conflict to allow its suffix to be taken away. If the growth results in a mismatch of amino acid type or of alignment, then

```

m ← ∅ // matching, from G to G*
F ← {{v} | v ∈ V} // each v starts in its own fragment
Repeat until convergence:
  Choose at random a vertex u ∈ V with no successor in F
  Choose an edge (u, v) ∈ E, for some v, with probability
  according to score
  // Try to grow from u to v at current alignment
  Let f_u and f_v be the fragments in F containing u and v
  f_u ← f_u + suffix of f_v starting at v
  f_v ← prefix of f_v before v
  If f_v is empty, remove it from F
  If m(v) is defined and m(u) is undefined and
  f_u can be aligned ending at m(v) - 1
    Update m to align f_u, i.e., m(u) ← m(v) - 1, etc.
  Else if m(u) is defined and m(v) is undefined and
  f_v can be aligned starting at m(u) + 1
    Update m to align f_v, i.e., m(v) ← m(u) + 1, etc.
  Else
    // Try to realign
    Let f = {p_1, ..., p_n} be the fragment with u and v
    Choose an alignment f' = [i, i + n] starting from
    position i, with probability according to score
    If any portion of f' already has some other fragment
    aligned there
      Choose to splice that out or to keep it,
      with probability according to score
    Update m
    Recursively handle spliced-out subfragments,
    if they are large enough and can be aligned

```

**Fig. 2.** Randomized algorithm for contact replacement: given a contact graph  $G^* = (V^*, E^*)$  and NMR graph  $G = (V, E)$ , determine the matching  $m$ .

a realignment is attempted. Matching the fragment somewhere else in the contact graph may result in a consistent matching, or may produce another conflict, potentially fixed by replacing part of the conflicting fragment with the new fragment. To keep each step simple enough, we only recursively handle the conflict at this point if it’s simple enough to fix. The algorithm repeats until convergence. In practice, we run a fixed number of iterations, and keep track of  $m$  through the iterations in order to analyze the distribution of good solutions.

At several places in the algorithm, we choose an option “with probability according to its score.” In general, the score refers to the total score of NMR edges matched to contact graph edges (refer again to the graph definition for our scoring function). Since we are using discrete amino acid classes, we require that the matched contact amino acid type be a member of the NMR amino acid class. In choosing an edge from  $u$ , we only consider the edges along the current path, while in choosing an alignment or whether or not to splice, we consider the total of all edges before vs. after the possible change.

## 5 RESULTS

Tab. 1 summarizes the datasets, both experimental and synthetic, that we used to validate our algorithm. The proteins are of moderate size for typical NMR studies, and this collection has representative structural diversity and assignment difficulty. We used three experimental datasets from previous contact-based assignment work (Kamisetty *et al.*, 2006; Xiong and Bailey-Kellogg,



**Fig. 3.** Reuse-based growing and aligning. Contact graph and NMR residues in the same column are matched. There are two amino acid types (empty squares and filled circles), which must match. (left) Growing from a matched fragment ending in  $u$  to an unmatched fragment with  $v$  in the middle leaves behind the prefix of the unmatched fragment in order to append and match the suffix following  $u$ . (right) Growing from  $u$  to  $v$  requires a realignment of the joined fragment. The joined fragment displaces the suffix starting at  $w$  of another fragment.

2007), including Human Glutaredoxin (PDB ID: 1JHB), Core Binding Factor  $\beta$  (PDB ID: 2JHB), and the catalytic domain of GCN5 histone acetyltransferase (PDB ID: 5GCN). For brevity, and since assignment is based on structure, we refer to each protein by its PDB ID. The noise rate (average number of noisy NMR edges per contact edge) is as high as 5.4 (1JHB  $\alpha$ -helices) and the missing rate as high as 51.8% (5GCN loops). Since such complete experimental datasets are a rare commodity, in order to more broadly test our approach, we also used a set of previously-generated synthetic datasets (Xiong and Bailey-Kellogg, 2007) based on chemical shift data deposited in the BMRB. These synthetic datasets include noise edges according to Gaussian noise with variance 0.02 (corresponding to a standard  $0.05 \text{ }^1\text{H}$  match tolerance) and missing edges according to observed statistics correlating the missing probability with the interatomic distance (Doreleijers *et al.*, 1999):  $d \leq 3 \text{ \AA}$ , missing 21%;  $3 < d \leq 4 \text{ \AA}$ , missing 41%.

For each dataset, we ran our algorithm 100 times, each for 10,000 iterations. For each run, we kept the top-scoring assignment over the 10,000 iterations. We then took as our solution ensemble the top 10 assignments over the 100 runs. For validation purposes, we use deposited solutions, which were determined by expert spectroscopists, as “reference” assignments.

For all test cases, the randomized algorithm took from twenty minutes to a few hours for the assignment of a *whole* protein. The time required depends on the quality of the input NMR data and of the structure—noisier datasets and less-representative structures take longer, as the search space is not as well constrained.

Fig. 4 illustrates some examples of the convergence of the algorithm; other runs and other datasets had similar behavior. In general, the score increases rapidly over the initial iterations (a few hundred steps). During this phase, pseudoresidues are being organized into various “short” paths aligned to the primary sequence, naturally increasing the score. With successive iterations, the short paths will start to grow into each other and conflicts occur, requiring fix-up moves to remove the conflicts. While moves are made so as to prefer increased score, locally bad moves are occasionally made in order to escape local optima. In many cases, the score converges to a value near that of the reference solution. As we will see below, the variation tends to produce only minor ambiguity in the resulting correspondence, and over the ensemble of solutions the correct assignments tend to be found.

Fig. 5 illustrates the assignment results for the experimental datasets. Notice that we can assign the *whole* protein, and that for most of the positions, the reference assignments are included in the top-ranked solutions. Exceptions tend to be from areas with many missing edges (e.g. 1JHB 51–57) or residues close to a Proline (e.g. 5GCN 34–35), which necessarily induces a break. The results also show that the high-scoring solutions tend largely to agree. For 1JHB,

there are on average 1.7 matches for each residue in  $\alpha$ -helices, and 1.2 in  $\beta$ -sheets and loops. For 2JHB the ambiguity level is 1.3 for  $\alpha$ -helices, 2.5 for  $\beta$ -sheets, and 2.4 for loops, and for 5GCN we have 1.3, 2.6, and 3. (These numbers can be compared to the expected number of matches *a priori*, which is simply the number of residues in the protein within the same ambiguous amino acid class, anywhere from 2 to 14.) In general,  $\beta$ -sheets and loops are more ambiguous than  $\alpha$ -helices since their tertiary structures generate fewer edge constraints. For the nine synthetic datasets, the average ambiguity is as low as 1 for  $\alpha$ -helices (1G6J),  $\beta$ -sheets (1KA5) and loops (1EGO); with a maximum of 2.8 (1SGO), 3.6 (1YYC), 9.1 (1SGO), and median of 1.7 (1KA5), 1.5 (1G6J), 2.1 (1G6J) for the three types, respectively. The most ambiguous case is 1SGO loops since it has both the highest noise ratio (6.3) and the largest RMSD (9.6  $\text{\AA}$ ).

We compared these results to the corresponding ones of (Bailey-Kellogg *et al.*, 2005) (limited to  $\alpha$ -helices), and found that our algorithm performs much better. Considering each position separately, we can evaluate how frequently the majority of the solution ensemble identifies the correct match. In our results, that is true for 90% of the positions, where it holds for less than 70% of the positions under the earlier method.

For both the experimental datasets and the synthetic ones, we studied the sensitivity of our algorithm to structural variation. For each dataset, an ensemble of NMR-determined structures had been deposited. We generated a contact graph for each different member of the ensemble, and studied how well the original data could be assigned under the varying structures. The average RMSDs of the ensemble members (all to the reference model) are given as the far right column in Tab. 1, and are representative of the extent of structural uncertainty one might expect when assigning NMR data using an x-ray structure or high-quality homology model.

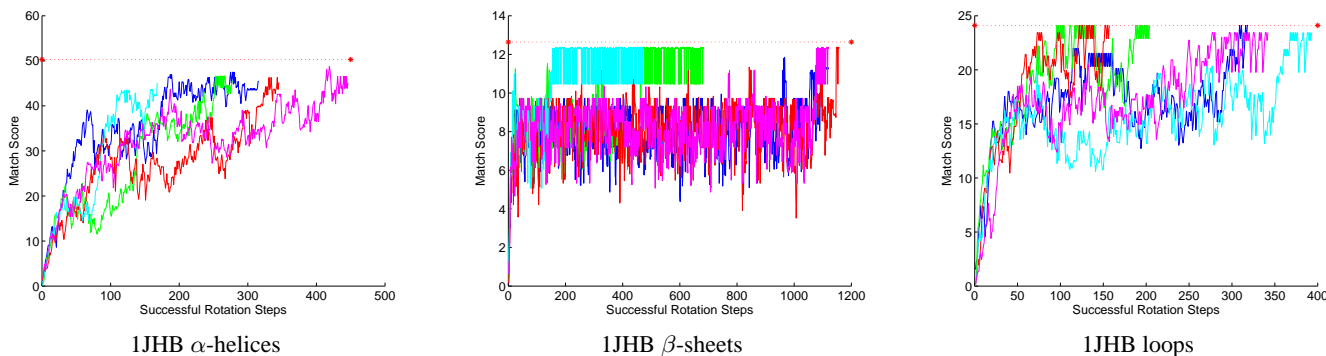
Fig. 6 illustrates the effect of structural variation on the performance of our algorithm for each secondary structure type. For experimental data, we observe that for  $\alpha$ -helices, there is no obvious change in the assignment accuracy when reference structures have a moderate difference (RMSD  $\leq 2 \text{ \AA}$ ). However, for  $\beta$ -sheets and loops, the assignment accuracy degrades when RMSD increases beyond about 1.25  $\text{\AA}$  for  $\beta$ -sheets and 3  $\text{\AA}$  for loops. Similar results can be observed in the synthetic data set— $\alpha$ -helices are very tolerant to structural uncertainty, while  $\beta$ -sheets are best for RMSDs under around 1.5  $\text{\AA}$ , and loops are best up to around 3.5  $\text{\AA}$ .

Fig. 7 summarizes the performance of our algorithm for each dataset under different structure models. These results suggest that, overall, we achieve good accuracy in assignment, above 80% for  $\alpha$ -helices, 70% for  $\beta$ -sheets and 60% for loops. Since contacts are discrete, one might expect more effects from structural variation. However, recall that our method focuses on matching paths

**Table 1.** Datasets (top 3 experimental; bottom 9 synthetic)

PDB ID	BMRB Entry	$\alpha/\beta/loop$					
		# elements	# residues	# edges	noise ( $\times$ )	missing (%)	RMSD ( $\text{\AA}$ )
1JHB	N/A	5/4/10	43/18/44	160/49/81	5.4/2.5/3.0	32.5/38.7/33.3	1.3/0.8/1.6
2JHB	4092	5/6/11	36/42/64	138/99/141	3.5/5.2/3.7	33.3/18.2/41.1	1.5/0.9/2.6
5GCN	4321	4/7/12	56/52/58	245/115/110	4.9/4.6/2.2	32.7/28.7/51.8	1.5/1.6/3.5
1KA5	2030	3/4/8	40/23/25	162/56/58	3.2/2.8/1.9	21, 41	0.8/0.7/0.8
1EGO	2152	3/4/8	39/19/27	165/42/49	2.2/2.7/2.6	21, 41	2.1/1.4/3.6
2FB7	7084	-/5/6	-/32/63	-/74/96	-/3.0/2.4	21, 41	-/1.5/7.7
1G6J	5387	2/5/8	18/22/36	75/47/71	1.4/3.1/3.0	21, 41	1.0/1.1/2.3
1P4W	5615	5/-/6	66/-/33	253/-/29	3.8/-/2.7	21, 41	1.2/-/3.5
1SGO	6052	4/6/9	47/26/64	199/68/131	2.9/3.4/6.3	21, 41	2.8/1.3/9.6
1RYJ	5106	1/5/7	9/27/37	31/55/51	1.0/4.3/3.4	21, 41	1.3/1.4/2.6
2NBT	1675	-/3/4	-/16/50	-/36/108	-/1.0/2.9	21, 41	-/1.5/4.5
1YYC	6515	2/9/11	36/72/66	149/165/153	1.2/4.7/2.6	21, 41	2.0/1.7/6.2

Columns give number of secondary structure elements, number of residues, number of contact graph edges, average number of noisy NMR edges per contact edge, percentage of missing contact edges and average RMSD to the reference model among structures in the deposited ensemble. Each column is broken into statistics for  $\alpha$ -helices,  $\beta$ -sheets, and loop regions, separated by slashes. ‘-’ indicates no instance of that secondary structure.

**Fig. 4.** Score convergence over 10,000 iterations for 5 individual test runs for 1JHB. Here a “successful” step indicates that a move has been accepted (a partial move can be rejected during fix-up). The dashed horizontal line at the top indicates the score of the reference assignment.

and uses non-sequential edges for scoring. While the score degrades with the loss of non-sequential edges, path connectivity is fairly well maintained regardless of the three-dimensional coordinates.

## 6 CONCLUSION

NMR spectroscopy provides scientists with the ability to collect detailed information regarding protein dynamics and interactions in solution. However, in order to interpret the dynamics and interaction experiments, it is necessary to first obtain a resonance assignment so that the observed spectral peaks may be matched to atoms in the protein (e.g., to localize which atoms are affected by binding). In order to increase the throughput and decrease the expense of performing resonance assignment, this paper develops a new approach, *contact replacement*. Contact replacement exploits information from an available three-dimensional structure (from x-ray crystallography or homology modeling) to drive the assignment process, replacing the typical more extensive and expensive set of experiments with a minimalist set. Once contact replacement has been performed, the

available assignments can be used to interpret dynamics or perturbation experiments. We note that those are separate experiments not included in the assignment process, and it is an interesting question (regardless of the assignment approach) to propagate uncertainty from assignment to uncertainty in dynamics or interactions.

Contact replacement poses interesting algorithmic problems in matching corrupted graphs, along with basic questions regarding the information content in connectivity and in vertex labels. In this paper we presented the first efficient algorithm to solve this problem for entire proteins. We used a random-graph theoretic framework to derive a theoretical justification for why our approach works well in practice. Even with a large number of noisy edges (a constant number per vertex) and a high degree of vertex label ambiguity, the random structure of the noise and ambiguity allows a polynomial-time algorithm to uncover the correct solutions.

We showed that our approach works quite well in practice, tolerating significant noise (up to 500% noisy edges), missings (up to 40%), and structural variability (up to 2  $\text{\AA}$  in  $\alpha$ -helices and  $\beta$ -sheets, and more in loops), while achieving very good assignment accuracy

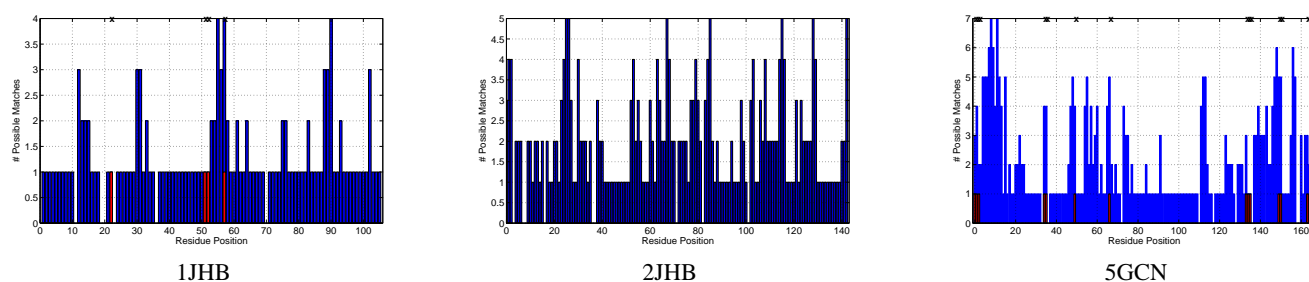


**Fig. 5.** Assignment ambiguity for experimental data sets. The bars indicate how many pseudoresidues can be mapped to each residue in the top 10 solutions. The red bars (also marked by 'X's at the top) indicate positions for which the reference assignment was not present in any solution.

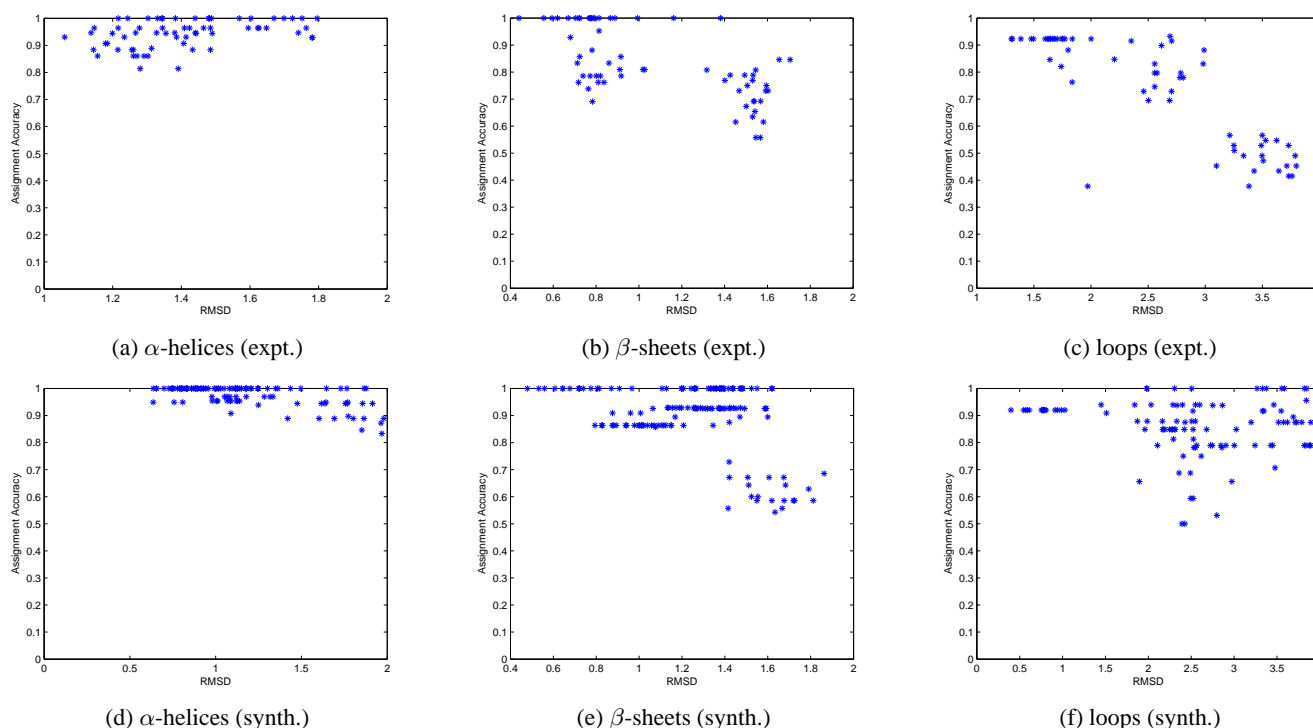


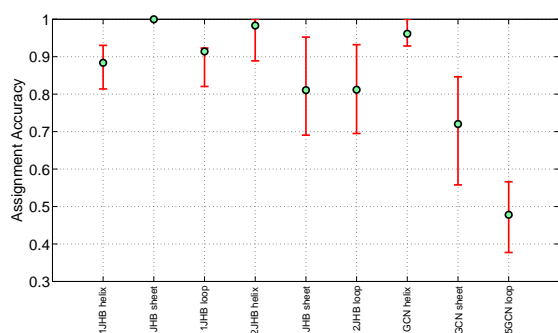
**Fig. 6.** Performance of our algorithm with varying structure, measured in terms of Root Mean Square Distance (RMSD) to the reference model. Each blue asterisk indicates the accuracy of one member of the structural ensemble for one dataset. We only show results for structures with at most 2 Å RMSD for  $\alpha$ -helices and  $\beta$ -sheets and 4 Å for loops.

(60–80% overall). This combination is quite promising, and a significant advance in the state of the art. In particular, our robustness to structural uncertainty suggests that we may even be able to handle a “looser” structural profile, such as the overall relationship among the core elements. This is a compelling challenge for further work.

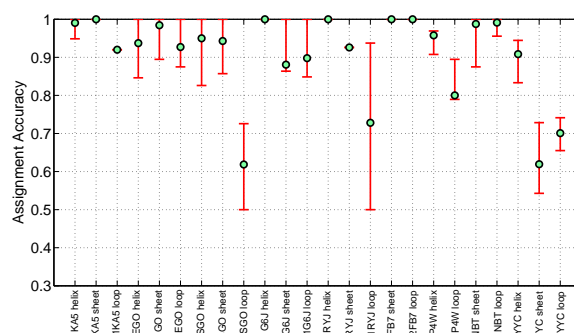
It is interesting to consider the relationship between contact replacement and nuclear vector replacement (NVR) (Langmead and Donald, 2004; Langmead *et al.*, 2004), both of which use an available structure to perform NMR resonance assignment, but based primarily on different data. (NVR does use some NOESY data, too, but only unambiguously assignable peaks.) At a high level, the residual dipolar coupling data used in NVR is global, giving orientations of bond vectors with respect to a coordinate frame, whereas the NOESY data used here is local, giving distances only between

close protons. A natural avenue of work is to study the relative information content of these types of information in order to develop a unified framework incorporating both.

Compared to other graph-based structure matching problems (e.g., threading, structural alignment, structure motif finding, chemical compound querying, etc.), contact replacement has no sequential order information for one of the graphs (the NMR one). However, the basic insights behind our algorithm (namely reusing partial solutions by making local fix-ups) may still be quite relevant in developing new algorithms for those applications. Alternatively, giving up sequential order in those applications may result in finding more distant relationships.



(a) experimental datasets



(b) synthetic datasets

**Fig. 7.** Overall performance of our algorithm. Cyan circles indicate average assignment accuracy over all members of an ensemble for a dataset, while bars indicate the best and worst assignments.

## ACKNOWLEDGMENTS

This work is supported in part by US NSF grant IIS-0444544 to CBK.

## REFERENCES

- Bailey-Kellogg, C., Widge, A., Kelley III, J., Berardi, M., Bushweller, J., and Donald, B. (2000). The NOESY Jigsaw: Automated protein secondary structure and main-chain assignment from sparse, unassigned NMR data. *J. Comp. Bio.*, **7**, 537–558.
- Bailey-Kellogg, C., Chainraj, S., and Pandurangan, G. (2005). A random graph approach to NMR sequential assignment. *J. Comp. Bio.*, **12**, 569–583.
- Bartels, C., Güntert, P., Billeter, M., and Wüthrich, K. (1997). Garant—a general algorithm for resonance assignment of multidimensional nuclear magnetic resonance spectra. *J. Comp. Chem.*, **18**(1), 139–149.
- Bjorklund, A., Husfeldt, T., and Khanna, S. (2003). Approximating longest directed path. *Electronic Colloquium on Computational Complexity*, **32**.
- Bollobas, B. (2001). *Random Graphs*. Cambridge University Press.
- Chen, Y., Reizer, J., Saier Jr., M., Fairbrother, W., and Wright, P. E. (1993). Mapping of the binding interfaces of the proteins of the bacterial phosphotransferase system, HPr and IIAGlc. *Biochemistry*, **32**, 32–37.
- Doreleijers, J., Raves, M., Rullmann, T., and Kaptein, R. (1999). Completeness of NOEs in protein structures: A statistical analysis of NMR data. *J. Biomol. NMR*, **14**, 123–132.
- Erdmann, M. and Rule, G. (2002). Rapid protein structure detection and assignment using residual dipolar couplings. Technical Report CMU-CS-02-195, School of Computer Science, Carnegie Mellon University.
- Feder, T. and Motwani, R. (2005). Finding large cycles in hamiltonian graphs. In *Proceedings of the ACM-SIAM Symposium on Discrete Algorithms (SODA)*.
- Feder, T., Motwani, R., and Subi, C. (2002). Approximating the longest cycle problem in sparse graphs. *SIAM J. Comput.*, **31**, 1596–1607.
- Gabow, H. N. (2004). Finding paths and cycles of superpolylogarithmic length. In *Proceedings of the 36th ACM Symposium on the Theory of Computing (STOC)*, pages 407–416.
- Garey, M., Johnson, D., and Tarjan, R. (1976). The planar hamiltonian circuit problem is np-complete. *SIAM J. Comput.*, pages 704–714.
- Güntert, P., Saltzmann, M., Braun, D., and Wüthrich, K. (2000). Sequence-specific NMR assignment of proteins by global fragment mapping with program Mapper. *J. Biomol. NMR*, **17**, 129–137.
- Hajduk, P., Meadows, R., and Fesik, S. (1997). Drug design: Discovering high-affinity ligands for proteins. *Science*, **278**, 497–499.
- Jung, J. and Zweckstetter, M. (2004). MARS - robust automatic backbone assignment of proteins. *J. Biomol. NMR*, **30**, 11–32.
- Kamisetty, H., Bailey-Kellogg, C., and Pandurangan, G. (2006). An efficient randomized algorithm for contact-based nmr backbone resonance assignment. *Bioinformatics*, **22**, 172–180.
- Kay, L. (1998). Protein dynamics from NMR. *Nat. Struct. Biol.*, **5 Suppl**, 513–517.
- Langmead, C. and Donald, B. (2004). An expectation/maximization nuclear vector replacement algorithm for automated NMR resonance assignments. *J. Biomol. NMR*, **29**, 111–138.
- Langmead, C., Yan, A., Lilien, R., Wang, L., and Donald, B. (2004). A polynomial-time nuclear vector replacement algorithm for automated NMR resonance assignments. *J. Comp. Bio.*, **11**, 277–298.
- Lin, G., Xu, D., Chen, Z.-Z., Jiang, T., and Xu, Y. (2002). A branch-and-bound algorithm for assignment of protein backbone NMR peaks. In *Proc. CSB*, pages 165–174.
- Montelione, G., Zheng, D., Huang, Y., Gunsalus, K., and Szyperski, T. (2000). Protein NMR spectroscopy in structural genomics. *Nat. Struct. Biol.*, **7 Suppl**, 982–985.
- Moseley, H. and Montelione, G. (1999). Automated analysis of NMR assignments and structures for proteins. *Curr. Opin. Struct. Biol.*, **9**, 635–642.
- Palmer III, A., Williams, J., and McDermott, A. (1996). Nuclear magnetic resonance studies of biopolymer dynamics. *J. Phys. Chem.*, **100**, 13293–13310.
- Pandurangan, G. (2005). On a simple randomized algorithm for finding a 2-factor in sparse graphs. *Information Processing Letters*, **95**(1), 321–327.
- Plesnik, J. (1979). The np-completeness of the hamiltonian cycle problem in planar digraphs with degree bound two. *Information Processing Letters*, **8**(4), 199–201.
- Pons, J. and Delsuc, M. (1999). RESCUE: An artificial neural network tool for the NMR spectral assignment of proteins. *J. Biomol. NMR*, **15**, 15–26.
- Pristovsek, P., Ruterjans, H., and Jerala, R. (2002). Semiautomatic sequence-specific assignment of proteins based on the tertiary structure—the program st2nmr. *J. Comp. Chem.*, **23**, 335–340.
- Rossmann, M. and Blow, D. (1962). The detection of sub-units within the crystallographic asymmetric unit. *Acta Cryst.*, **15**, 24–31.
- Shuker, S., Hajduk, P., Meadows, R., and Fesik, S. (1996). Discovering high-affinity ligands for proteins: SAR by NMR. *Science*, **274**, 1531–1534.
- Vitek, O., Vitek, J., Craig, B., and Bailey-Kellogg, C. (2004). Model-based assignment and inference of protein backbone nuclear magnetic resonances. *Statistical Applications in Genetics and Molecular Biology*, **3**, article 6, 1–33. <http://www.bepress.com/sagmb/vol3/iss1/art6/>.
- Vitek, O., Bailey-Kellogg, C., Craig, B., Kuliniewicz, P., and Vitek, J. (2005). Reconsidering complete search algorithms for protein backbone NMR Assignment. *Bioinformatics*, **21**, ii230–236.
- Vitek, O., Bailey-Kellogg, C., Craig, B., and Vitek, J. (2006). Inferential backbone assignment for sparse data. *J. Biomol. NMR*, **35**, 187–208.
- Xiong, F. and Bailey-Kellogg, C. (2007). A hierarchical grow-and-match algorithm for backbone resonance assignments given 3D structure. In *Proc. IEEE BIBE*, pages 403–410.
- Xu, Y., Xu, D., Crawford, O., Einstein, J., and Serspersu, E. (2000). Protein structure determination using protein threading and sparse NMR data. In *Proc. RECOMB*, pages 299–307.
- Zimmerman, D., Kulikowski, C., Huang, Y., Feng, W., Tashiro, M., Shimotakahara, S., Chien, C., Powers, R., and Montelione, G. (1997). Automated analysis of protein NMR assignments using methods from artificial intelligence. *J. Mol. Biol.*, **269**, 592–610.